Downloaded from orbit.dtu.dk on: May 05, 2023

DTU Library

Multi-omic profiling of EPO-producing Chinese hamster ovary cell panel reveals metabolic adaptation to heterologous protein production

Ley, Daniel; Kazemi Seresht, Ali; Engmark, Mikael; Magdenoska, Olivera; Nielsen, Kristian Fog; Kildegaard, Helene Faustrup; Andersen, Mikael Rørdam

Published in:
Biotechnology and Bioengineering

Link to article, DOI:
10.1002/bit.25652

Publication date:
2015

Document Version
Publisher's PDF, also known as Version of record

Link back to DTU Orbit

Citation (APA):
Ley, D., Kazemi Seresht, A., Engmark, M., Magdenoska, O., Nielsen, K. F., Kildegaard, H. F., & Andersen, M. R. (2015). Multi-omic profiling of EPO-producing Chinese hamster ovary cell panel reveals metabolic adaptation to heterologous protein production. *Biotechnology and Bioengineering*, *112*(11), 2373-2387. https://doi.org/10.1002/bit.25652

General rights
Copyright and moral rights for the publications made accessible in the public portal are retained by the authors and/or other copyright owners and it is a condition of accessing publications that users recognise and abide by the legal requirements associated with these rights.

- Users may download and print one copy of any publication from the public portal for the purpose of private study or research.
- You may not further distribute the material or use it for any profit-making activity or commercial gain
- You may freely distribute the URL identifying the publication in the public portal

If you believe that this document breaches copyright please contact us providing details, and we will remove access to the work immediately and investigate your claim.

ARTICLE

BIOTECHNOLOGY and BIOENGINEERING

Multi-Omic Profiling of EPO-Producing Chinese Hamster Ovary Cell Panel Reveals Metabolic Adaptation to Heterologous Protein Production

Daniel Ley,[1,2,3] Ali Kazemi Seresht,[2] Mikael Engmark,[1,2] Olivera Magdenoska,[1] Kristian Fog Nielsen,[1] Helene Faustrup Kildegaard,[3] Mikael Rørdam Andersen[1]

[1]Department of Systems Biology, Technical University of Denmark, Kongens Lyngby, Denmark; telephone: +45-45-25-26-75; fax: +45-45-88-41-48; e-mail: mr@bio.dtu.dk

[2]Cell Culture Technology, Novo Nordisk A/S, Novo Nordisk Park, Måløv, Denmark

[3]The Novo Nordisk Foundation Center for Biosustainability, Technical University of Denmark, Hørsholm, Denmark

ABSTRACT: Chinese hamster ovary (CHO) cells are the preferred production host for many therapeutic proteins. The production of heterologous proteins in CHO cells imposes a burden on the host cell metabolism and impact cellular physiology on a global scale. In this work, a multi-omics approach was applied to study the production of erythropoietin (EPO) in a panel of CHO-K1 cells under growth-limited and unlimited conditions in batch and chemostat cultures. Physiological characterization of the EPO-producing cells included global transcriptome analysis, targeted metabolome analysis, including intracellular pools of glycolytic intermediates, NAD(P)H/NAD(P)$^+$, adenine nucleotide phosphates (ANP), and extracellular concentrations of sugars, organic acids, and amino acids. Potential impact of EPO expression on the protein secretory pathway was assessed at multiple stages using quantitative PCR (qPCR), reverse transcription PCR (qRT-PCR), Western blots (WB), and global gene expression analysis to assess EPO gene copy numbers, EPO gene expression, intracellular EPO retention, and differentially expressed genes functionally related to secretory protein processing, respectively. We found no evidence supporting the existence of production bottlenecks in energy metabolism (i.e., glycolytic metabolites, NAD(P)H/NAD(P)$^+$ and ANPs) in batch culture or in the secretory protein production pathway (i.e., gene dosage, transcription and post-translational processing of EPO) in chemostat culture at specific productivities up to 5 pg/cell/day. Time-course analysis of high- and low-producing clones in chemostat culture revealed rapid adaptation of transcription levels of amino acid catabolic genes in favor of EPO production within nine generations. Interestingly, the adaptation was followed by an increase in specific EPO productivity.

Biotechnol. Bioeng. 2015;112: 2373–2387.

© 2015 Wiley Periodicals, Inc.

KEYWORDS: Chinese hamster ovary; erythropoietin; chemostat; metabolomics; transcriptomics; metabolic adaptation

Introduction

Most biopharmaceutical products like monoclonal antibodies, hormones, and blood-related proteins are produced in Chinese hamster ovary (CHO) cells (Walsh, 2014). Studies of CHO cells have yielded a basic understanding of mammalian cell biology and driven the development of mammalian cell factories for production of structurally advanced pharmaceutical glycoproteins (Jayapal and Wlaschin, 2007). For example, numerous studies have focused on resolving bottlenecks in the protein production and secretory pathway (i.e., transcription, translation, protein translocation, -folding, -modification and -secretion), which limit the cell-specific protein productivity (Kim et al., 2012). Often the production bottleneck is reported to be independent of the heterologous target protein, indicating a general limitation of the secretory protein processing capacity (Jossé et al., 2012), while in some cases the bottleneck is linked to the synthesis of a specific post-translational protein modification (Pybus et al., 2013).

In brief, protein production bottlenecks in CHO cells have been reported at the level of transgene expression (Jiang et al., 2006; Lee et al., 2009a; Mason et al., 2012) and stability of mRNA transcripts (Hung et al., 2010). Numerous studies report a non-linear correlation between mRNA copy numbers and specific protein secretion, indicating limitations of either mRNA translation or post-

Daniel Ley and Ali Kazemi Seresht contributed equally to the work.
Author contributions: D.L. performed part of the experimental work, developed new analysis methods, analyzed data and wrote the manuscript. A.K.S. performed part of the experimental work, analyzed data and wrote the manuscript. M.E performed part of the experimental work, analyzed data and wrote the manuscript. O.M. developed new methods, performed part of the experimental work and wrote the manuscript. K.F.N. developed new methods and analyzed data. HFK performed part of the experimental work and wrote the manuscript. M.R.A. wrote the manuscript.
The authors declare no conflict on interest.
Correspondence to: M.R. Andersen
Contract grant sponsor: Novo Nordisk Foundation
Contract grant sponsor: Lundbeck Foundation
Received 14 January 2015; Accepted 11 May 2015
Accepted manuscript online 20 May 2015;
Article first published online 30 June 2015 in Wiley Online Library (http://onlinelibrary.wiley.com/doi/10.1002/bit.25652/abstract).
DOI 10.1002/bit.25652

© 2015 Wiley Periodicals, Inc.

translational processes (Chusainow et al., 2009; Lattenmayer and Loeschel, 2007; Lattenmayer et al., 2007; Mead et al., 2009; O'Callaghan et al., 2010; Reisinger et al., 2008). One study suggests that the translocation of mRNA to the endoplasmatic reticulum (ER) is limiting protein production in CHO cells (Kang et al., 2014). Other studies have reported bottlenecks in protein folding capacity for specific proteins (Borth et al., 2005; Chung et al., 2004; Hwang et al., 2003; Lee et al., 2009b; Mohan and Lee, 2010). Furthermore, some studies have found bottlenecks within vesicular transport of proteins from ER to the Golgi apparatus and within exocytotic transport from the trans-Golgi cisternae to the plasma membrane (Peng and Fussenegger, 2009; Peng et al., 2011). Finally, for specific glycoproteins, evidence suggest bottlenecks in the processing of N-linked glycan structures (Bolt et al., 2008). In general, all major steps (i.e., transcription, translation, protein translocation, protein folding, protein glycosylation, and inter-organelle protein transport) have been argued to be a bottleneck. In many cases, it is possible that the cultivation method is confounding the analysis, as one could expect that different cultivation modes (batch, fed-batch, continuous, various forms of nutrient starvation) will have varying requirements for native protein production, and thus influence the metabolic load on the cell.

Cultivation of recombinant cells is performed in different ways, depending on the goal of the experiment. In batch cultivation, all nutrients are supplied initially in excess, allowing growth at maximum specific rate with maximum specific nutrient uptake and maximum production of native proteins. In an industrial context, the batch process is of limited use for protein production, since growth and productivity rapidly becomes limited by nutrient availability and by-product inhibition. As an alternative process, where growth, by-product accumulation and nutrient consumption can be controlled, continuous cultures are operated with a constant in-flow of fresh medium, while spent medium, biomass and product is removed at an equal rate. A popular continuous cultivation format for physiological characterization of cells is the chemostat (Bull, 2010), which is operated at a constant dilution rate (i.e., rate of medium flow per culture volume), thus ensuring a constant physiochemical environment in the bioreactor. This feature enables the study of effects of single parameters on the cell physiology. Moreover, the restricted in-flow of fresh medium allows tight control of the growth rate of cultivated cells as availability of nutrients becomes limiting in the culture. The operation at a fixed dilution rate thus enables the normalization of growth rates between parallel cultures, which has been shown to be a prerequisite for global transcriptional profiling as the expression level of many genes is affected by the specific growth rate (Regenberg et al., 2006). Chemostat cultures have been used extensively as a powerful tool for the study of, for example, metabolism, protein production, genetic stability, and long-term metabolic adaptation of micro-organisms (comprehensively reviewed by Bull, 2010). However, so far only a few studies have described the physiological characterization of CHO cells in chemostat culture (Hayter et al., 1992, 1993; Lee et al., 1998; Nyberg et al., 1999).

The 'omics technologies (e.g., genomics, transcriptomics, proteomics, metabolomics, glycomics and fluxomics) provide systems-level data on the intracellular state of a biological system crucial to elucidate the molecular basis of CHO cell physiology (reviewed by Kildegaard et al., 2013). Comparative analysis of 'omics data gathered under specific physiological conditions has revealed differentially regulated molecular mechanisms responsible for desirable phenotypes in isogenic clone populations and guided the design of improved cell factories (Chong et al., 2010; Sengupta et al., 2011; Smales et al., 2004; Yee et al., 2009).

The metabolic burden imposed by heterologous protein production in mammalian cells is still not well characterized and thus may offer opportunities for further improvement of protein productivity. A recent study by Niklas et al. (2013) comparing human cells expressing α_1-antitrypsin found increased anabolic demand for RNA and lipids in protein producers and argued that such a phenotype could be caused by increased transcriptional load and expanded ER associated with secretory protein production. By simulating the theoretical metabolite demand using a network model, they linked the metabolic changes in protein producing cells to increased C1-unit, nucleotide and lipid metabolism, which led to specific adaptations in the amino acid metabolism and increased secretion of glycine and glutamate. The authors concluded that C1 and lipid metabolism seem important targets for improvement of protein production in mammalian cells.

The glycoprotein hormone erythropoietin (EPO) is a commonly used model protein in development of CHO-based bioprocesses (Choi et al., 2007; Sung et al., 2004; Surabattula et al., 2011; Yoon et al., 2005) and metabolic engineering of CHO cells for improved protein production (Kim et al., 2004, 2011). The typical EPO expression levels from clones with no gene amplification are reported in the range of 1–10 pg/cell/day (Kim and Lee, 2009; Yoon et al., 2003; Zhou et al., 2010), which is substantially lower than, for example, antibody production processes.

The aim of the current study was to discover bottlenecks in EPO production in CHO cells and characterize the burden of heterologous protein production under growth dependent and independent conditions. For this, a panel of stably EPO expressing CHO-K1 clones spanning a 25-fold productivity range was established and characterized in batch and chemostat cultures. We employed a multi-omic physiological characterization including NMR-based metabolic footprinting (exo-metabolome) of sugars, organic acids and amino acids, LC-MS based metabolite fingerprinting (endo-metabolome) of glycolytic intermediates, NAD(P)H/$NAD(P)^+$ and ANPs. Quantitative PCR (qPCR), quantitative reverse transcription PCR (qRT-PCR), Western blots (WB), and affymetrix CHO microarrays were used to assess EPO gene copy numbers, EPO gene expression, intracellular protein levels and genome-wide gene expression analysis of differentially expressed genes functionally related to secretory protein processing, respectively.

Materials and Methods

Cell Lines and Media

The EPO-expressing cell lines were developed from the ATCC (Manassas, Virginia) CHO-K1 line cat no. CCL-61. Prior to cell line development the parental cell line was adapted for suspension and serum-free culture in a complex animal-component free Novo Nordisk proprietary medium supplemented with 4 mM L-glutamine (Thermo Scientific, Waltham, MA). During development of EPO-

expressing cell lines the media were supplemented with 2.5 mL anti clumping agent (Invitrogen, Carlsbad, CA) per 1 L medium and penicillin–streptomycin mix (Invitrogen) in concentrations of 100 U/mL of penicillin and 100 μg/mL streptomycin. 600 μg/mL Geneticin/G418 (Invitrogen) was applied as selection pressure 1 day after transfection and throughout the cell line generation process.

Primers

Primers for uracil-specific excision reagent (USER) cloning procedure (Table I) were designed according to the USER cloning design scheme in (Lund et al., 2014) and purchased from Integrated DNA Technologies (Leuven, Belgium). Primers for specific amplification of target sequences in hEPO, β-actin (Actb) and glyceraldehyde-3-phosphate dehydrogenase (Gapdh; Table I) were designed using the online quantitative PCR primer design tool from Roche (Basel, Switzerland), which is based on the Primer3 software (Untergasser et al., 2012) and gene sequences were retrieved from www.chogenome.org (Hammond et al., 2012).

Chemicals for Analysis of Intercellular Metabolites

Isotope-labeled standards were purchased from Silantes Gmbh (München, Germany). All other standards of metabolites were obtained from Sigma–Aldrich (St. Louis, MO), except for acetyl coenzyme A that was produced by Santa Cruz Biotechnology (Dallas, TX). High purity solvents and reagents were used in order to reduce the background noise from impurities as much as possible. The solvents acetonitrile and methanol used for extraction were HPLC grade from Sigma–Aldrich while the methanol used for chromatography was LC-MS grade from Fluka. All water was milli-Q purified. The ion pair reagent tributylamine (TBA; HPCL grade) was from Sigma–Aldrich, while the acetic acid (LC-MS grade) was from Fluka.

Plasmid Construction

A vector plasmid pEPO-NEOR was assembled using the USER based FAST-mediated vector assembly procedure as previously described (Lund et al., 2014). Neomycin resistance was included in the construct as selection marker. The human erythropoietin (EPO) gene (Powell and Berkner, 1986) in the plasmid construct was codon-optimized for CHO and synthesized from Geneart (Regensburg, Germany). The mammalian expression vector pU0002 (Hansen et al., 2011) harboring an *Escherichia coli* origin of replication element and an ampicillin resistance gene was used as plasmid backbone. The EPO gene was under control of the human cytomegalovirus (CMV) promoter and flanked by the bovine growth hormone polyadenylation signal (BGHpA), while the NEO^R gene was regulated by the simian vacuolating virus 40 (SV40) promoter and polyadenylation signal (SV40pA). USER elements harboring promoter regions, polyadenylation signals, the NEO^R gene, and the protein backbone were produced exploiting PCR primers and protocols from (Lund et al., 2014). Analogously, a USER element with EPO was prepared using the uracil-containing primers found in Table I. The NEO^R gene was assembled with its promoter and polyadenylation signal in one USER cloning event exploiting the USER enzyme mix (New England Biolabs) and the competent *E. coli* DH5α strain (Invitrogen, Carlsbad, CA) as described in details in (Lund et al., 2014). Subsequently, the formed selection marker element was amplified by PCR and used in a second USER cloning procedure for generation of the vector plasmid pEPO-NEOR. Plasmid sequence was verified by sequencing (Star SEQ, Mainz, Germany).

Generation of EPO-Expressing Cell Lines

Transfection of the parental CHO-K1 cell line with the plasmid vector pEPO-NEO^R was performed by electroporation in a BioRad GenePulser Xcell set to deliver a single pulse of 900 μF at 300 V and infinity resistance in a 4 mm cuvette. As positive control a subset of cells were transfected with a mammalian expression vector with the gene for enhanced green fluorescent protein (eGFP) and neomycin resistance. The control transfection was used to estimate transfection efficiency, follow cell death, clone expansion, and transgene expression. Prior to each transfection 40 μg of plasmid DNA was added directly to the cuvette containing 10^7 cells in growth medium. Twenty-four hours after transfection G418 selection pressure was added and the transfected cells were split into two. Single clones were isolated from one half of the transfected cells in a limiting dilution experiment with twenty 96-well plates containing either 500 or 1,000 transfected cells/well. During 2 weeks of cultivation one 96-well plate was exposed to microscope inspection daily to observe initial cell death and stable clones expanding. From the untouched 96-well plates circular monoclonal cultures were screened for EPO production using a dot blot procedure followed by WB and enzyme-linked immunosorbent assay (ELISA; see below) and expanded further.

Table I. List of primers and corresponding sequences used for quantitation of gene copy numbers and gene expression levels.

Primer name	Target gene	Purpose	Primer sequence 5′–3′
EPO-Fwd	*hEPO*	Copy number determination	AGAGGCCGAGAACATCACCA
EPO-Rev	*hEPO*	Copy number determination	CCCACTTCCATCCGCTTA
GAPDH-Fwd	*Gapdh*	Copy number determination	AGCTTGTCATCAACGGGAAG
GAPDH-Rev	*Gapdh*	Copy number determination	ATCACCCCATTTGATGTT
ActB-Fwd	*Actb*	Copy number determination	CCAGCACCATGAAGATCAAG
ActB-Rev	*Actb*	Copy number determination	TGCTTGCTGATCCACATCTC
EPO (CHO optimized)-Fwd	*hEPO*	Plasmid construction	AGTGCGAUATGGGCGTGCACGAGTGTC
EPO (CHO optimized)-Rev	*hEPO*	Plasmid construction	AGACTGTGUTAATCTATCGCCGGTCCGGC

The second half of the transfected cells were maintained as a polyclonal shake flask culture for 3 weeks. For the first 2 weeks the culture volume was gradually decreased in each passage to maintain a viable cell density of 0.3×10^6 cells/mL. Single clones were isolated from the polyclonal culture by limiting dilution into 384-well plates and robot-assisted single clone selection in a Cello system (TAP Biosystems, Royston, UK). The cells were cultivated and photos were taken for 13 days with medium change every 6 days. Single clone cultures were screening for EPO production and scaled up to 30 mL shake flask cultures.

Screening Cell Lines for EPO Production

Isolated monoclonal cell lines were screened for EPO production using WB and selected clonal cultures were up-scaled and evaluated further using the Quantikine IVD ELISA kit (R&D Systems, Minneapolis, MN) following the manufacturer's protocol.

The Invitrogen NuPAGE system was used for WB. Samples of culture supernatant were drawn and centrifuged at 15,000*g* for 1 min and treated following the NuPage guidelines for preparation of reduced samples and peptide *N*-glycosidase treated samples using PNGases F (New England Biolabs, Ipswich, MA). Samples were run at 12% NuPAGE Novex Bis–Tris mini gels with MOPS running buffer in an Xcell SureLock mini cell at 200 V (constant) for 45 min with MagicMark^{TM} XP Western protein standard (Invitrogen) and Full-range rainbow molecular weight marker (GE Healthcare). Gel separated proteins were transferred by an Invitrogen iBlot device to a nitrocellulose membrane with 0.45 μm pore size (Invitrogen). 2.0% TBS–T, was used as blocking buffer and for washing steps 0.5% TBS–T was employed. The membrane was incubated with 1 μg/mL polyclonal rabbit anti-EPO antibody (AbCam, Cambridge, UK) in 10 mL 0.5% TBS–T at room temperature with gentle shaking at 45 rpm for 45 min. Following three washing steps with 0.5% TBS–T the membrane was incubated with 0.2 μg/mL IRDye 680 goat anti-rabbit (Li-Cor Biosciences) fluorescent labeled secondary antibody in 0.5% TBS–T for 45 min with shaking at 45 rpm. The membrane was analyzed in a Li-Cor Odyssey infrared imaging system. Supernatant from eGFP clones served as negative control.

Cell Culture

Cell culture was performed in vented Erlenmeyer shake flasks (Corning, NY) in a shaking incubator operated at 36.5°C, 5% CO_2 and 140 rpm. Cells were cultured in repeated batch cultivation during the development of EPO-expressing cell lines. The cells were passaged twice a week and the viable cell density was adjusted to 0.3×10^6 cells/mL.

Pre-cultures were initiated from frozen cells and cultivated as above, but without selection pressure. The pre-cultures were passaged every other day to ensure growth at maximum specific growth rate.

Bioreactor Cultivation and Analysis

Parental and recombinant CHO-K1 cells were cultivated in 1.5 L bioreactors (Eppendorf DASGIP multi-fermentor system, Jülich, Germany) with a working volume of 1 L. Temperature was maintained at 36.5°C with an agitation rate of 200 rpm using two three-way segmented impellers. Dissolved oxygen was maintained at 50% of air saturation using air, O_2 and CO_2 operated at a constant flow rate of 0.6 L/h. Culture pH was maintained at 7.15 with a deadband of 0.25 using intermittent CO_2 addition to the gas mix and 2 M sodium carbonate. Culture pH and pO_2 was measured on-line and calibrated to an offline reference RAPIDpoint 500 blood gas analyzer (Siemens Healthcare Diagnostics, Erlangen, Germany) subsequent to inoculation. Cell number, viability, cell size and aggregation was measured using a CedeX HiRes (Roche), extracellular concentrations of glucose, lactate, glutamine, glutamate, and ammonium was measured with a Bioprofile 100^{PLUS} (Nova Medical, Waltham, MA). Supernatant samples for extracellular EPO quantitation were stored at −80°C until HPLC analysis.

Batch cultures were seeded with 0.3×10^6 cells/mL and samples were drawn on a daily basis and analyzed for cell density, viability, cell size, and aggregation rate. Extracted culture supernatants were analyzed for glucose, lactate, glutamine, glutamate, ammonium, EPO, pH, pO_2, and pCO_2. Genomic DNA was extracted after 48 h and analyzed for EPO gene copy numbers by quantitative PCR. The culture was terminated after 160 h.

Chemostat cultures were seeded with 0.3×10^6 cells/mL and chemostat cultivation mode was initiated 72 h subsequent to inoculation with a constant dilution rate of 0.3 volumes/day. The cultures were sampled daily and analyzed for cell density, viability, cell size, and aggregation rate. The supernatant was analyzed for glucose, lactate, glutamine, glutamate, ammonium, EPO, pH, pO_2, and pCO_2. Samples for metabolic footprinting were analyzed for amino acids, sugars, and organic acids by quantitative NMR analysis (Spinnovation Biologics, Nijmegen, Netherlands). Genomic DNA and RNA was extracted and analyzed for EPO gene copy number and EPO gene expression level by qPCR and qRT-PCR, respectively. Selected cultures were subjected to microarray based gene expression analysis.

HPLC Quantitation of Erythropoietin

EPO from thawed supernatant samples was quantified by RP-HPLC on an Agilent 1200 using an XBridge C8 $4.6 \times 150\ mm^2$ (3.5 μm) column (waters), operated at 42°C and a flow rate of 1 mL/min. Buffer A was composed of 0.1% TFA in milliQ water and buffer B was composed of 0.07% TFA in acetonitrile. The elution gradient consisted of 30–70% buffer B over 16 min. Protein detection was performed by UV light absorption at 214 nm and EPO concentration was determined using human erythropoietin (Cell Signaling, Danvers, MA) as standard.

Preparation of DNA, RNA, and cDNA

Genomic DNA (gDNA) was isolated from pellets of 3×10^6 CHO cells using a DNAeasy blood and tissue genomic DNA purification kit (Qiagen, Hilden, Germany) following the manufacturers instructions. DNA concentration and purity was determined using a Nanodrop 8000 (Thermo Scientific, Wilmington, DE). Samples with $A_{260/280}$ ratios ≥ 2 were considered to be of sufficient purity.

For total RNA isolation, 3 mL culture sample was extracted and centrifuged at 900*g* for 5 min. The supernatant was discarded and

the cell pellet was homogenized in 2 mL Trizol reagent (Invitrogen) and stored at −80°C. Total RNA was extracted using an RNA plus mini kit (Qiagen) according to the manufacturer's instructions including column-based digestion of DNA. Total RNA quantity was determined spectrophotometrically using a Nanodrop 8000 (Thermo Scientific) and RNA sample integrity was determined using an Agilent 2100 Bioanalyzer (Agilent, Santa Clara, CA) ensuring RIN values above 9.0.

cDNA was generated from total RNA using a High Capacity cDNA Reverse Transcription kit (Applied Biosystems, Foster city, CA) according to the manufacturers instructions.

Determination of Relative *hEPO* Gene Copy Numbers and mRNA Levels

Relative EPO transgene copy numbers and mRNA levels were determined using real-time quantitative PCR on gDNA and mRNA, respectively. Primer pairs were tested for specificity and amplification efficiency. Primer dimerization and specificity was investigated using melting curve analysis, which revealed a single thermal transition confirming that the primers were specific for the target genes and indicating absence of primer dimerization. Standard curves were generated from serial dilutions of pooled gDNA in triplicates and amplification efficiencies close to 100% were achieved for all primer pairs. Primers targeting the commonly used reference genes *Gapdh* and *Actb* were screened for amplification efficiency and *Gapdh* was selected as reference gene as the primers produced amplification efficiencies closer to 100%. Quantitative PCR was performed using a QuantiFast SYBR Green PCR Kit (Qiagen) containing the fluorescent dye SYBR green I and ROX as fluorescent reporter. Quantification of relative EPO gene dosage and expression level was carried out in 384-well plates in a 7900HT FAST Real-Time PCR System (Applied Biosystems) with a reaction volume of 10 μL. All PCR reactions were run in triplicates. The assay was executed with the following thermal profile: 10 min heat activation of the polymerase at 95°C followed by 40 amplification cycles consisting of DNA dissociation at 95°C for 5 s and primer annealing at 60°C for 20 s. The dissociation stage consisted of a linear temperature ramp from 60°C to 95°C over the course of 10 min. The C_T values were computed using the AutoC_T algorithm found in the software package SDS 2.4 (Applied Biosystems). For calculation of gene copy numbers cells were assumed to be diploid.

Transcriptomics Sample Preparation and Data Analysis

Chemostat cultivations of three clones (clones 1, 4, and 7) were carried out in two parallel cultures (biological replicates) and samples for RNA isolation were taken during the steady-state phase of each culture, as determined by constant concentrations of medium components (amino acids and sugars). RNA samples were isolated from the culture as described above. RNA sample integrity was determined using Agilent 2100 Bioanalyzer and RNA 6000 Nano LabChip kit (Agilent), ensuring RIN values above 9.0, and total RNA quantity was determined with a NanoDrop 3300 UV–Vis spectrophotometer (Thermo Scientific, Rockford, IL). Using the GeneChip Hybridization, Wash and Stain Kit, the probe preparation and hybridization to affymetrix CHO gene 2.0 ST arrays were performed according to manufacturer's instructions (Affymetrix GeneChip Expression Analysis). Washing and staining of arrays were performed using the GeneChip Fluidics Station 450 and scanning with the Affymetrix GeneArray 3000 7G Scanner (Affymetrix, Santa Clara, CA). The Affymetrix GeneChip Command Console Software (AGCC) was used to generate CEL files of the scanned arrays.

Differential gene expression analysis was performed using the transcriptome analysis console (TAC) 2.0 (Affymetrix) software package using one-way ANOVA, P values were corrected for multiple comparisons by Benjamini and Hochberg False Discovery Rate (FDR). Transcripts with a FDR P value <0.05 were considered statistically significant.

Western Blot Analysis of Intracellular EPO Retention

Intracellular EPO retention was examined using SDS–PAGE in conjunction with WB analysis. Intracellular proteins were extracted from pellets of 5×10^6 cells in mid-exponential phase using 1 mL Mammalian Protein Extraction Reagent with complete™ protease inhibitor cocktail added (Thermo Scientific). The mixture was left to react for 10 min with gentle shaking and cell debris were removed by centrifugation at 14,000*g* for 15 min. For electrophoresis, 28 μL total protein sample was denatured with 4 μL NuPage Sample Reducing Agent (Invitrogen) and 8 μL NuPage LDS Sample Buffer (Invitrogen) at 80°C for 5 min and size fractionated on a 12% NuPAGE Novex Bis–Tris mini gel with MOPS running buffer. Gel separated proteins were transferred to a 0.45 μm pore size nitrocellulose membrane using an iBlot (Invitrogen), mouse anti-EPO (R&D Systems) was used as primary antibody and a fluorescent labeled donkey anti-mouse antibody (Licor) was used as secondary antibody. The fluorescence was quantified using an Odyssey CLx (Licor) with human erythropoietin (Cell Signaling) as positive control.

Quenching and Extraction of Intracellular Metabolites

For analysis of intracellular metabolite pools, 10^7 cells were extracted from mid-exponential batch cultures and immediately quenched with four sample volumes 0°C 0.9% w/v NaCl on ice (inspired by Dietmair et al., 2010). The cooled cell suspension was immediately spun down at 1,000*g* for 1 min at 0°C and the supernatant discarded. One milliliter of −79°C methanol was added to the cell pellet followed by addition of an internal standard mixture containing 10 μg/mL of [U-^{13}C] ATP and [U-^{13}N] AMP and flash freezing in liquid nitrogen (inspired by Sellick et al., 2010). Samples were stored at −80°C before thawing on ice and two successive extractions were performed with 1 mL 50% v/v acetonitrile in water (inspired by Dietmair et al., 2010). The extraction procedure included addition of solvent solution, resuspension of cell pellet by vortexing, incubation on ice for 10 min and separation of cell debris and liquid phase by centrifugation at 4,200*g* for 5 min. The pooled extraction supernatants were filtered through a 0.45 μm teflon syringe filter Ø17 mm (National Scientific, Rockwood, TN). Eight milliliter acetonitrile was added to the filtrate to facilitate water evaporation

before drying under nitrogen atmosphere at room temperature. The extracted metabolites were dissolved in 150 μL milliQ water containing 10 mM tributylamine and 10 mM acetic acid resulting in a final concentration of 1 μg/mL of each of the internal isotope-labeled standards. Prior to the analysis the samples were filtrated using a 0.45 μm teflon syringe filter Ø17 mm (National Scientific).

Ion-Pair Liquid Chromatography Tandem Mass Spectrometry

All LC-MS/MS experiments were performed on an Agilent 1290 Infinity LC coupled with an Agilent 6460 triple quadrupole MS analyser equipped with electrospray ionization source. The MS was operated in negative multiple reaction monitoring (MRM) mode.

Ten microgram/millilter single standard solutions in 10 mM TBA and 10 mM acetic acid were used to optimize the compound specific MS and ion source parameters. The two most intense MRM transitions for each metabolite were determined in a direct infusion experiment using a KDS100 infusion pump with a flow rate of 9.8 μL/min. Then, for each chosen MRM transition the collision energy (CE), fragmentor and cell accelerator voltages (CAV) were optimized by injecting 1 μL of 10 μg/mL single standard solutions. When investigating the optimal compound specific parameters for the MS/MS analysis, the following range of voltages were tested: fragmentor voltage 90–130 V in steps of 10 V, CE 5–35 V in steps of 5 V and CAV 3 and 4 V. The MRMs used for the analysis are given in Supplementary Materials. The best compound specific parameters were those giving the most intense LC-MS peak. The ion source dependent parameters were as follows: gas temperature 300°C; sheath gas temperature 400°C; nebulizer gas flow rate 8 L/min; nebulizer pressure 50 psi; and capillary voltage 4,500 V. Nitrogen was used as collision gas. The entrance potential (ΔEMV) and dwell time were kept at 500 and 30 ms, respectively, for all transitions.

The chromatographic separation was obtained on a Luna 2.5 μ C18(2)-HST (100 × 2.0 mm^2) HPLC column (Phenomenex, Aschaffenburg, Germany) operated at 40°C. Eluent A was water containing 10 mM tributylamine and 10 mM acetic acid and eluent B was 90% (v/v) methanol containing 10 mM tributylamine and 10 mM acetic acid. The gradient was stepwise 0–5 min, 0% B; 5–10 min, 0–2% B; 10–11 min, 2–9% B; 11–16 min, 9% B; 16–24 min, 9–50% B; 24–28 min, 50% B; 28–28.5 min, 50–100% B; 28.5–30 min, 100% B; 30–30.5, 100–0% B; 30.5–36 min, 0%. The final 5.5 min were used for equilibration of the column prior to the next run. The flow rate was 0.3 mL/min and the sample injection volume was set to 5 μL.

One milligram/milliliter single standard stock solutions in water were used to prepare 10 μg/mL mixture of the compounds of interest in eluent A. The latter mixture was used to prepare the calibration solutions with concentrations ranging from 0.05 to 10 μg/mL. Standard curves used for the quantification were constructed by plotting the peak area of the compounds against the concentration. For the compounds for which internal standards were available the calibration curves were constructed by plotting the ratio of the peak area of labeled and unlabeled compounds against their concentrations. A chromatogram of detected compounds in mammalian cell extracts is supplied in Supplementary Materials.

Metabolic Network Reconstruction

A draft network reconstruction of the glycolytic and amino acid catabolic pathways in CHO cells was generated using the mouse metabolic pathways as template. Biochemical pathway data from mouse metabolism was retrieved from the Kyoto Encyclopedia of Genes and Genomes database (Kanehisa and Goto, 2000; Kanehisa et al., 2014) and homologs gene sequences in the CHO genome were identified using the Chinese hamster genome database www.CHOgenome.org (Hammond et al., 2012). The draft network reconstruction was further refined by careful curation of gene–protein-reaction relationships using manual genome annotation and literature evidence. The finalized reconstruction featured 319 proteins catalyzing 183 reactions with 188 metabolites (metabolic map is supplied in Supplementary Materials).

Statistical Analysis

The statistical test for determination of physiological differences between clone populations was performed using Student's t test with a significance level of $\alpha = 0.05$.

Results

Cell Line Generation and Clone Selection

Seven single cell clones were selected based on proliferation rate and EPO expression to establish a panel of stable clones with specific EPO productivities (q_{EPO}) ranging from less than 0.2 to 5 pg/cell/day (determined in exponential growth phase), thus covering a 25-fold range of productivity (Fig. 1). All EPO producing clones and a non-transfected parental clone were adapted to the growth medium (Q-CM105) to exclude the influence of ongoing medium adaptation on physiological characterization. During the adaptation phase, clones were monitored for specific growth rate, specific glucose and glutamine uptake rates, specific lactate and

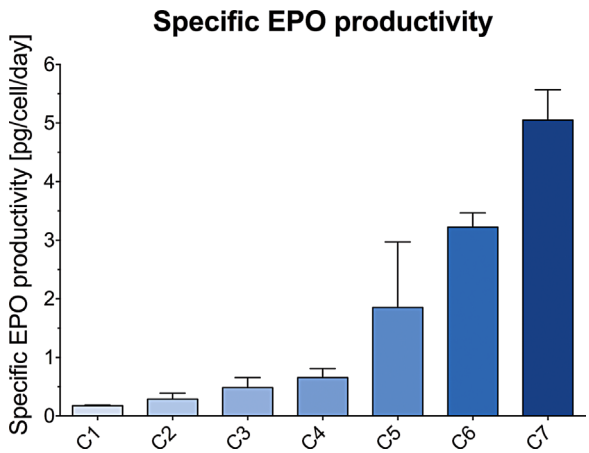

Figure 1. Specific EPO productivity. The error bars indicate standard deviation of two biological replicates.

ammonium secretion rates and specific EPO production rate. After 20 days in 100 mL repeated batch culture, all measured parameters had stabilized (i.e., remained within 7%). Thus, the clones were considered fully adapted to the growth medium and a master cell bank was established.

EPO Production Has No Effect Growth, Nutrient Uptake or By-Product Secretion

Clones C1-7 and the parental clone were physiologically characterized in duplicate batch cultivations in bioreactors under nutrient excess conditions, to ensure maximum specific growth rate (Supplementary Materials). To assess the physiological impact of EPO production, the control was compared to the EPO producing clones (data displayed in Table II). No significant difference was found in growth characteristics (i.e., specific growth rate and biomass yield), excluding major physiological stress from EPO production. An analysis of correlation (Supplementary Materials) between the cell phenotypic variation displayed in Table II and q_{EPO} was performed to identify patterns in clone physiology that might explain the difference in q_{EPO}. The analysis identified no correlations in the dataset (Table II), suggesting that an in-depth physiological analysis was required to discover phenotypic markers for high q_{EPO}.

Comparison Across EPO Producing Clones Reveals No Detrimental Effect on Glucose Metabolism

In order to assess possible metabolic impact of differential EPO expression on energy metabolism, we performed a quantitative characterization of intracellular metabolites related to glucose energy and redox metabolism (i.e., specific glycolytic intermediates, NAD(P)H/NAD(P)$^+$ and ANPs). For this, triplicate batch cultures of all EPO producing clones were sampled in parallel, during mid-exponential growth phase and metabolite profiles were generated using an extraction technique that does not differentiate between cellular compartments, thus picturing the average concentration of intracellular metabolites. The differences in concentrations of adenosine phosphates and nicotinamide adenine dinucleotides did not exhibit a marked correlation to q_{EPO} (linear regression analysis, $R^2 < 0.36$; Fig. 2A and C). The adenylate energy charge (AEC) ratio represents the amount of metabolically available energy stored in the adenine nucleotide pool (Atkinson, 1968). The catabolic and anabolic reduction charges represent the redox state of the cell (Andersen and von Meyenburg, 1977). The observed distributions (Fig. 2 B, D, and E) indicate that EPO production is not limited by insufficient energy availability from adenosine phosphates or nicotinamide adenine nucleotides (linear regression analysis, $R^2 < 0.36$).

Furthermore, intracellular concentrations of several carbon metabolites from glycolysis and acetyl coenzyme A were determined and compared between clones (Fig. 3). As observed for adenosine phosphates and nicotinamide adenine nucleotides, the differential q_{EPO} was not reflected in metabolite concentrations indicating that EPO production is not limited by glucose metabolism (linear regression analysis, $R^2 < 0.33$).

Chemostat Cultivation of Three EPO Producing Clones Show Temporal Correlations in Gene Expression and EPO Titer

To identify the bottleneck in the protein production pathway, three clones (C1, C4, and C7) were selected for an in-depth physiological characterization under growth-limited conditions in duplicate

Table II. Raw data obtained in duplicate batch cultivations of EPO producing clones (C1-C7) and the parental clone (Control) in bioreactors.

Clone	μ_{max} (day^{-1})	IVCD (10^6 cells*h/mL)	q_{Glc} (pmol/cell/day)	q_{Lac} (pmol/cell/day)	q_{Gln} (pmol/cell/day)	q_{Glu} (pmol/cell/day)	q_{NH4} (pmol/cell/day)	$Y_{Lac/Glc}$ (mol/mol)	$Y_{NH4/Gln}$ (mol/mol)	q_{EPO} (pg/cell/day)
C1	0.97/1.00	712/639	5.88/4.52	7.08/6.91	1.10/1.07	0.20/0.17	0.94/0.73	1.20/1.53	0.86/0.69	0.18/0.17
C2	0.91/1.05	627/587	6.73/5.28	7.14/7.59	0.96/1.05	0.16/0.16	0.8 /0.64	1.06/1.44	0.84/0.61	0.36/0.21
C3	0.70/0.81	446/456	5.78/5.57	7.88/9.20	0.92/0.97	0.21/0.30	1.01/0.90	1.36/1.65	1.09/0.92	0.60/0.36
C4	0.86/0.97	544/532	4.58/4.69	6.88/7.17	1.00/1.06	0.23/0.18	0.88/0.78	1.50/1.53	0.88/0.73	0.76/0.54
C5	0.80/0.81	308/254	6.56/7.30	10.7/10.9	1.63/1.50	0.33/0.28	1.50/1.16	1.63/1.50	0.92/0.77	2.64/1.06
C6	0.89/1.00	585/579	5.86/5.18	5.96/7.42	1.05/1.00	0.20/0.21	0.87/0.72	1.02/1.43	0.82/0.71	3.05/3.39
C7	0.89/0.97	584/500	4.62/6.07	7.74/8.80	1.17/1.22	0.29/0.24	0.87/0.88	1.68/1.45	0.83/0.72	4.66/5.42
Control	0.92/0.98	528/557	4.67/4.94	7.01/7.72	1.18/1.15	0.26/0.17	0.92/0.75	1.50/1.56	0.78/0.65	—

Clone	Glc/Gln consumption (mol/mol)	Cell size (μm)	Aggregation rate (%)
C1	5.36/4.26	13.41/13.30	29.52/15.85
C2	7.05/5.03	13.38/13.41	18.83/12.12
C3	6.27/5.73	13.05/12.90	25.85/11.97
C4	4.58/4.40	13.40/13.06	23.70/13.38
C5	4.02/4.87	16.25 / 16.01	35.04/32.18
C6	5.56/5.13	13.51/13.37	19.27/12.86
C7	3.95/4.96	13.94/13.69	20.03/8.61
Control	3.95/4.30	13.92/13.37	22.64/11.81

μ_{max}, maximum specific growth rate; IVCD, Integral of viable cell density (biomass yield); q_{Glc}, maximum specific glucose uptake rate; q_{Lac}, maximum specific lactate secretion rate; q_{GLN}, maximum specific glutamine uptake rate; q_{GLU}, maximum specific glutamate secretion rate; q_{NH4}, maximum specific ammonium secretion rate; $Y_{Lac/Glc}$, yield of lactate on glucose; $Y_{NH4/GLN}$, yield of ammonium on glutamine; q_{EPO}, specific EPO productivity; Glc/GLN consumption, uptake ratio of glucose/glutamine.

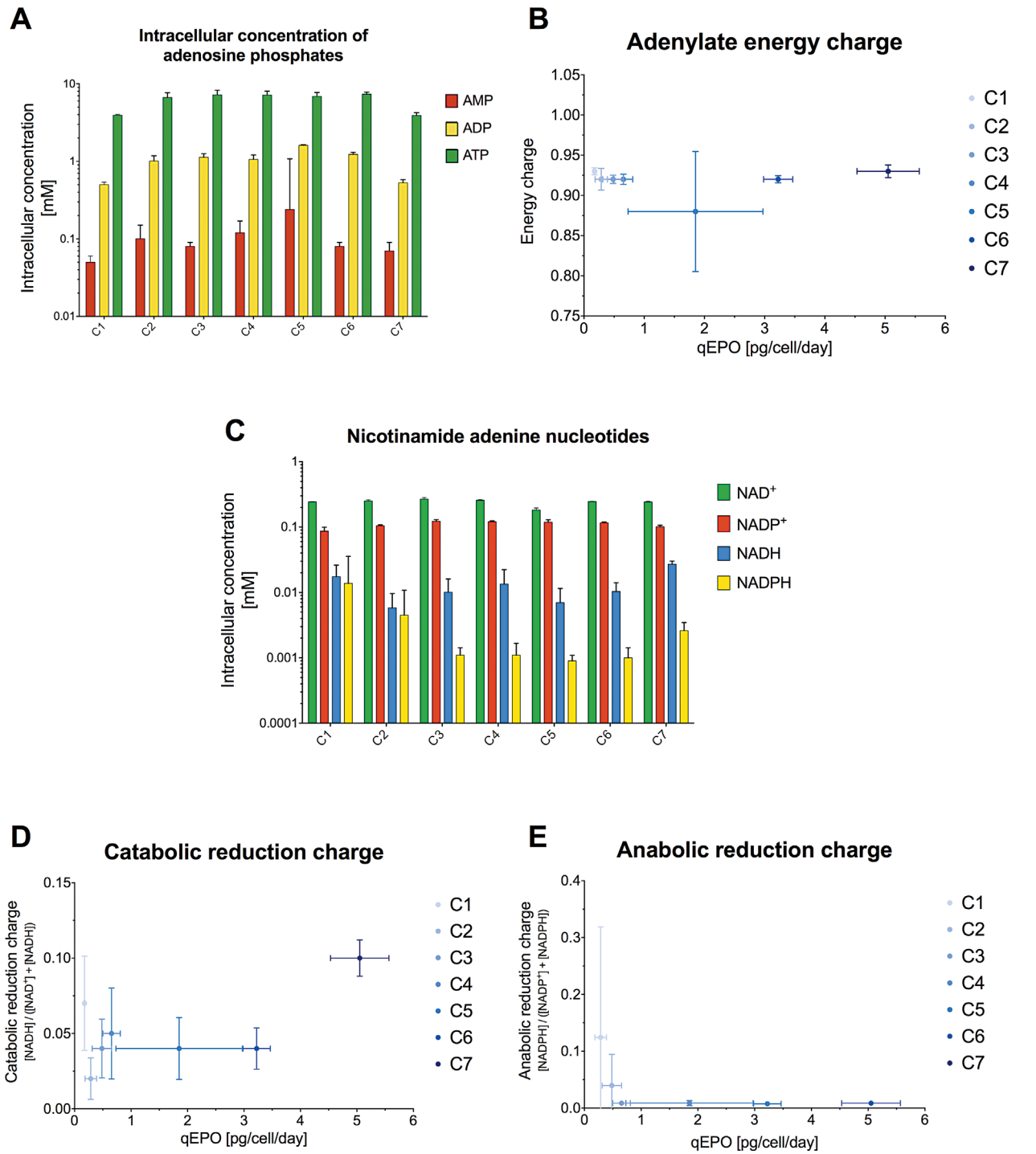

Figure 2. Overview of intracellular energy and redox-related metabolites in EPO clones. **A**: Intracellular concentration of adenosine phosphates. **B**: Adenylate energy charge. **C**: Intracellular concentration of phosphorylated and non-phosphorylated nicotinamide adenine dinucleotides. **D**: Catabolic reduction charge. **E**: Anabolic reduction charge. Error bars indicate standard deviation of three biological replicates.

chemostat cultivations. The cultures were continued for 31 days with a fixed specific growth rate of 0.3 day^{-1} corresponding to 15 generations at 30% of maximum growth rate. The chemostat cultivation mode was selected to normalize for growth-related effects on protein productivity across the three clones, thus unveiling physiological variation in protein production efficiency regardless of maximum growth capacity. The assumption was that normalization of the specific growth rate lead to normalization of metabolic fluxes and therefore picture the intrinsic metabolic efficiency of protein production between the clones. Samples were

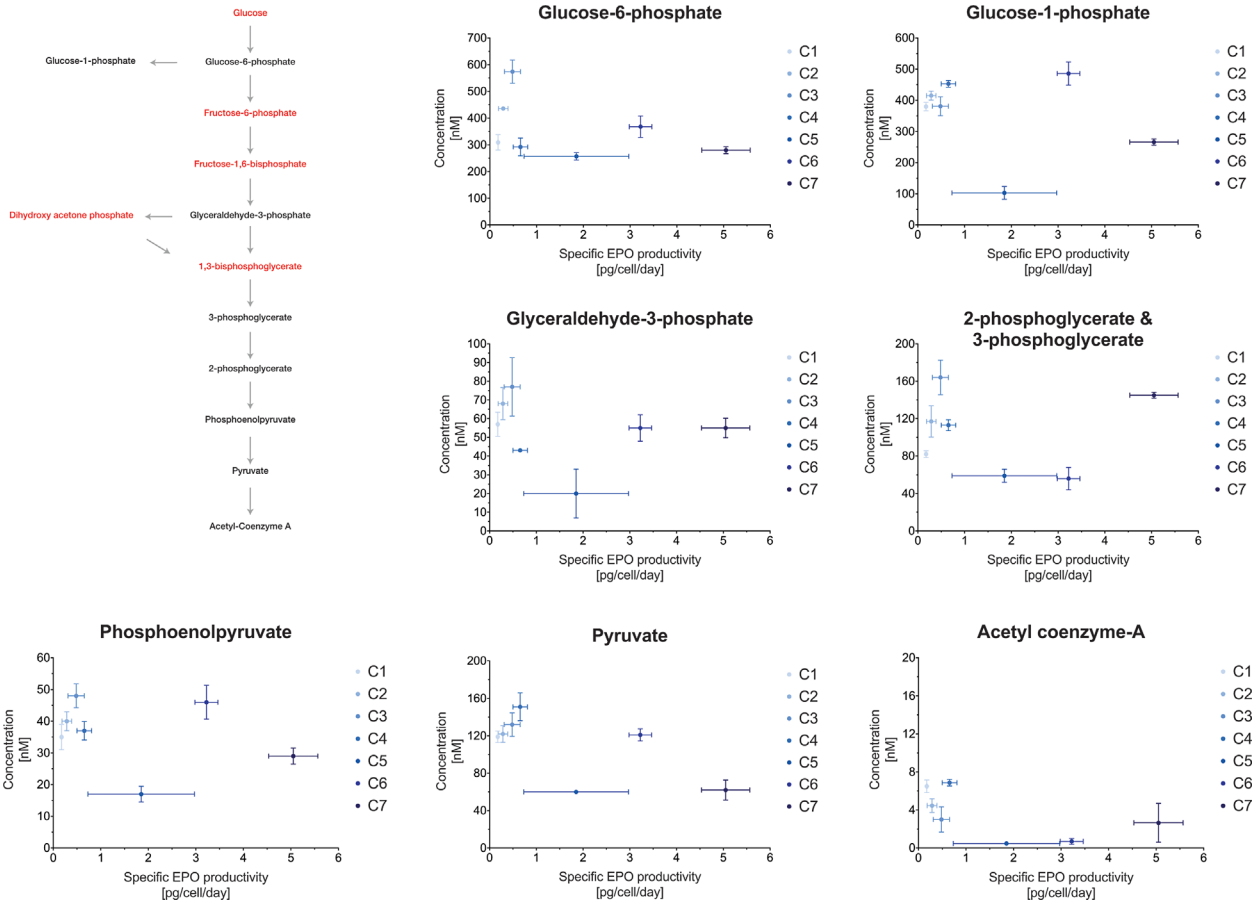

Figure 3. Schematic representation of glycolysis and associated levels of intracellular metabolites. Quantified metabolites are indicated with black font on the pathway map (left). The concentrations of 3-phosphoglycerate and 2-phosphoglycerate were pooled, as they could not be separated in the method. Error bars indicate standard deviation of three biological replicates.

taken daily from each chemostat culture and the secreted protein levels, EPO gene copy numbers, mRNA levels (Fig. 4) and amount of intracellular accumulated EPO were determined (Supplementary Materials). The viable cell density (Fig. 4A), stabilized at approximately 5 million cells/mL after 10 days. Analysis of spent growth medium suggested that the cultures reached steady-state at day 12, as concentrations of medium components (amino acids and sugars) and metabolic by-products (lactate and ammonium) were constant in all cultures from this time-point (Supplementary Materials). The dynamics of EPO titers pictures three distinct phases (Fig. 4B). In phase I (day 1–10) the EPO titers decrease as the cells adjust to the imposed growth limitation and the steady state. During phase II (day 10–20) the cells reach steady-state and protein titers are relatively stable in all cultures. In phase III (day 20–31) the EPO titers increase corresponding to an increase of q_{EPO} by 56%, 74%, and 83% for clone 1, clone 4, and clone 7, respectively, in phase III relative to phase II (Fig. 4E and F bars). The EPO gene copy numbers were determined by qPCR using relative quantitation with *Gapdh* as reference gene. The dynamics of EPO gene copy numbers feature a steady increase over the course of the cultivation (Fig. 4C). Starting with 1.5 relative EPO gene copies, the determined gene copy numbers slowly increase toward two EPO gene copies, suggesting a culture-average absolute EPO gene copy number of 3 at the beginning of the cultivation and 4 in the end. The dynamics of EPO gene expression pictured a decrease around day 12 consistent in all cultures (Fig. 4D). The basis of the sudden decrease is unknown, but the timing correlates with depletion of lactate in the growth medium. From day 20, the EPO gene expression increased in all clones throughout the cultivation, correlating well with the increased EPO titers in phase III.

Post-Transcriptional Protein Processing Efficiency of EPO in the Protein Secretory Pathway Correlates With Specific EPO Productivity Across Clones

For determination of differences in EPO transcription efficiency across clones, we compared the ratios of culture-average EPO gene expression per EPO gene, that is, the ratio of EPO mRNA to EPO gene (Fig. 4E). It was noticed that the transcriptional efficiency of clones 4 and 7 was identical throughout the experiment and that the transcriptional efficiency of clone 1 was consistently 20% lower than the other clones. To determine differences in post-transcriptional

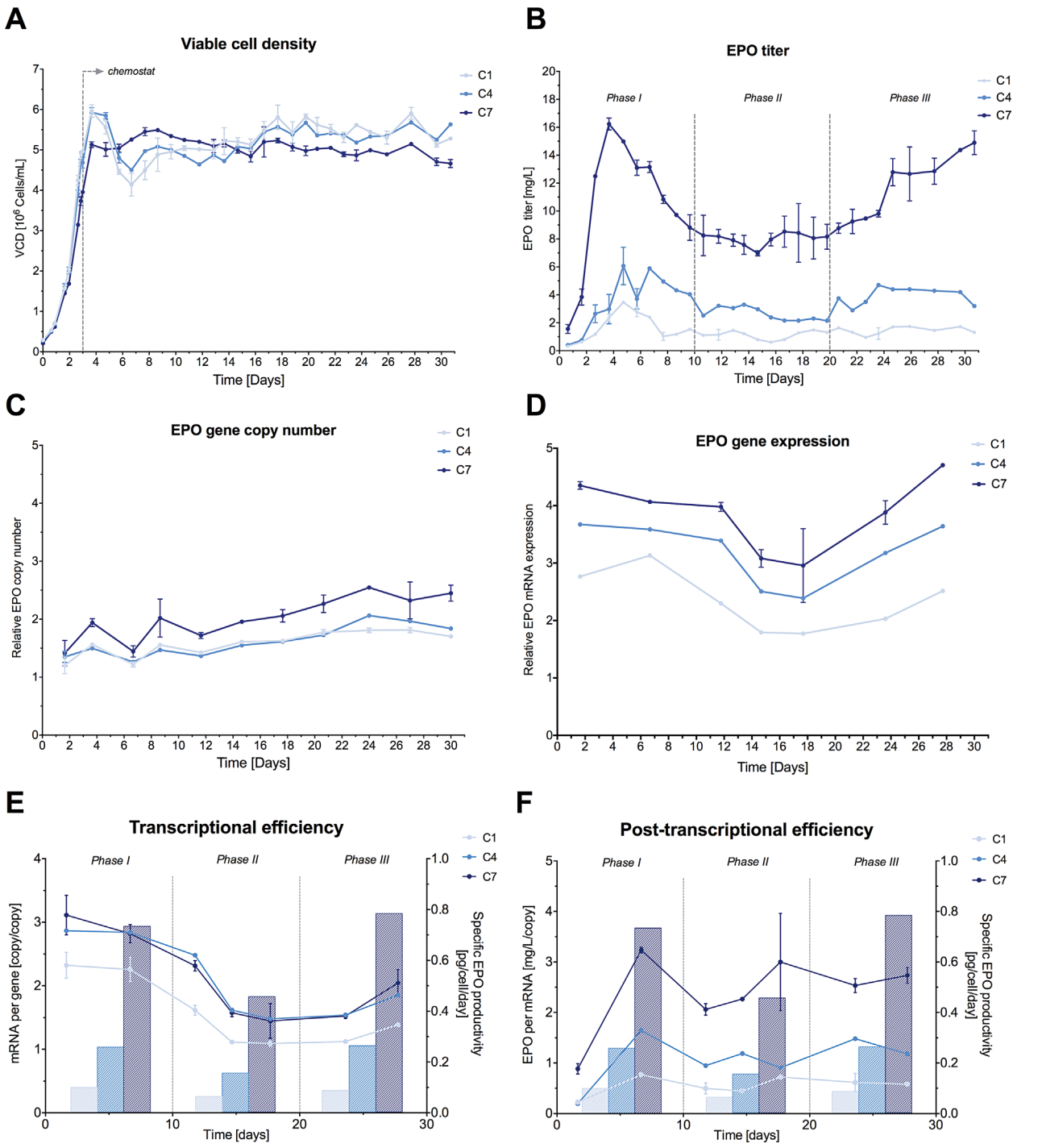

Figure 4. Culture dynamics of clones 1, 4, and 7 during 31 days of continuous culture in chemostat. **A**: Viable cell densities. **B**: Extracellular EPO titres. **C**: Determined EPO gene copy numbers. **D**: Determined EPO gene expression. **E**: Ratio of determined EPO mRNA transcript per EPO gene (curves) and averaged specific EPO productivity for phases I, II, and III (bars). **F**: Ratio of secreted EPO per mRNA transcript (curves) and averaged specific EPO productivity for phases I, II, and III (bars). Error bars indicate standard deviation of two biological replicates.

processing of EPO across the clones, we compared the culture-average ratios of EPO titer and EPO gene expression, that is, EPO titer per EPO mRNA, thus reflecting the efficiency of protein translation and secretory protein processing (protein folding, -maturation and -secretion) across clones (Fig. 4F). It was noticed that the post-transcriptional efficiency was significantly higher in clone 7 relative to clone 4 and clone 1 and corresponded well to the observed difference in q_{EPO}. Therefore, we investigated whether different amounts of EPO were retained intracellular in the clones. For this, total cellular protein extracts were separated using SDS–

PAGE and analyzed for EPO contents using WB (Supplementary Materials). The differences in intracellular EPO levels corresponded to the observed extracellular EPO titers (Fig. 4B) indicating that EPO is not retained intracellular in any clones.

Global Gene Expression Analysis Indicate Adaptation of Gene Expression Levels of Amino Acid Catabolic Genes to Preserve Most Abundant Amino Acids in EPO

To identify differentially expressed genes functionally related to secretory protein processing across the EPO producers we performed a global gene expression analysis comparing the highest and lowest EPO producers (clone 7 and clone 1, respectively) during the steady-state phase of chemostat culture in phase II (triplicate samples were generated from days 12, 15, and 18). The differential gene expression analysis identified no enrichment in the gene expression landscape of genes related to protein translocation, protein folding, protein glycosylation or vesicular transport (Supplementary Materials), indicating that neither of these processes were limiting the protein productivity. Next, we investigated whether the protein production bottleneck was reflected in differential expression of metabolic genes. For this analysis, we generated a network reconstruction of the glycolytic pathway and the amino acid catabolic pathways, as these are the most active catabolic pathways and thus most likely to limit energy metabolism (the reconstructed metabolic network is displayed in Supplementary Materials). The network reconstruction served as a framework for meaningful interpretation of the differential gene expression data on a pathway level. The results indicated a general up-regulation of glycolytic genes in clone 7, suggesting a possible increased energy demand in this clone. Interestingly, when inspecting the differential gene expression levels of amino acid catabolic genes, we discovered a tendency towards preservation of the most abundant amino acids in EPO in the high producer relative to the low producer (i.e., decreased transcription level of genes responsible for degradation of the amino acids most frequently found in EPO; Fig. 5). Specifically, 12 of the 13 most abundant and non-secreted amino acids in EPO had reduced expression of catabolic reactions in the high producer relative to the low producer (Fig. 5B). Thus, the result indicated possible regulatory adaptation of gene expression towards decreased amino acid catabolism specific for the most abundant amino acids in EPO, in the high producer relative to the low producer. It was noticed that the observation was followed by an increase of q_{EPO} by 56% and 83% in clones 1 and 7, respectively (phase III, Fig. 4B).

Discussion

Comparison Across EPO Producing Clones Revealed No Apparent Bottlenecks in the Protein Expression and Secretory Pathway or Energy Metabolism

The secretory production of proteins in CHO cells can be characterized as a cascade of protein modification and quality control steps catalyzing the post-translational processing of a nascent polypeptide into a functionally mature protein (Hussain et al., 2014). The overproduction of a heterologous protein increases the trafficking through the secretory pathway to the limit of the protein processing capacity leading to productivity bottlenecks. To increase the knowledge of the bottleneck associated with secretory production of EPO in CHO cells, we established a panel of CHO-K1 clones spanning a 25-fold range of specific EPO productivity and assessed the phenotypical differences at multiple stages within the protein expression and secretion pathway.

The comparison of transcriptional efficiency (Fig. 4E) showed a lower transcription rate per EPO gene in clone 1 compared to clone 4 and 7 throughout the experiment, indicating that the EPO gene was inserted in a locus with less transcriptional activity in clone 1. While clones 4 and 7 showed identical transcriptional efficiencies, the comparison of post-transcriptional efficiency (Fig. 4F) revealed that clones 1 and 4 were severely limited in EPO secretion per EPO transcript compared to clone 7 (23% and 50% of C7 at day 15, respectively). It was observed that the difference in post-transcriptional efficiency corresponded to the difference in q_{EPO} indicating that the expression bottleneck was enrooted downstream of transcription (i.e., translation, translocation, protein folding, -glycosylation and -transport). The differential EPO expression was not reflected in intracellular protein concentration as determined by WB, as this correlated well with the difference in extracellular protein concentration, indicating that post-translational processing of EPO in the secretory pathway is not a bottleneck. This indication was underlined by the fact that the global gene expression analysis of clones 1 and 7 found no significant (P values >0.05) difference in expression level of single genes or expression enrichment within a group of genes functionally related to secretory protein production (i.e., genes involved in translocation, protein folding, -glycosylation and -transport).

The determination of gene- and transcript levels during prolonged chemostat cultivation led to some noteworthy observations. The slightly increasing trend of EPO gene copy numbers was surprising. However, the effect may be explained by presence of a sub-population of cells with different copy numbers of *hEPO* or *Gapdh*, as previously demonstrated by Beckmann et al. (2012). Similarly, the sudden decrease of EPO transcripts around day 12 (Fig. 4D) was surprising. The basis of the decrease was unknown, but the timing in all five cultures correlated well with the depletion of lactate in the growth medium and may be associated with a metabolic shift.

It was investigated whether the differential EPO expression across the clones was caused by a bottleneck in carbon and/or energy metabolism. For this, intracellular metabolites were sampled in mid-exponential growth phase as this was assumed to picture the maximum metabolic capability of each clone. Comparison of intracellular concentrations of adenosine phosphates and nicotinamide adenine dinucleotides across clones showed no correlation to q_{EPO} (Fig. 2). This observation indicated that the energy metabolism was keeping up with the increased energy requirement in the EPO producing clones, which is in agreement with similar studies of other mammalian cell types (Khoo et al., 2007; Niklas et al., 2013). Furthermore, the lack of correlation between concentrations of glycolytic intermediates and q_{EPO} (Fig. 3) indicated that glucose metabolism was not limiting for EPO productivity in batch culture. However, in the chemostat culture, we observed a change in the expression landscape of

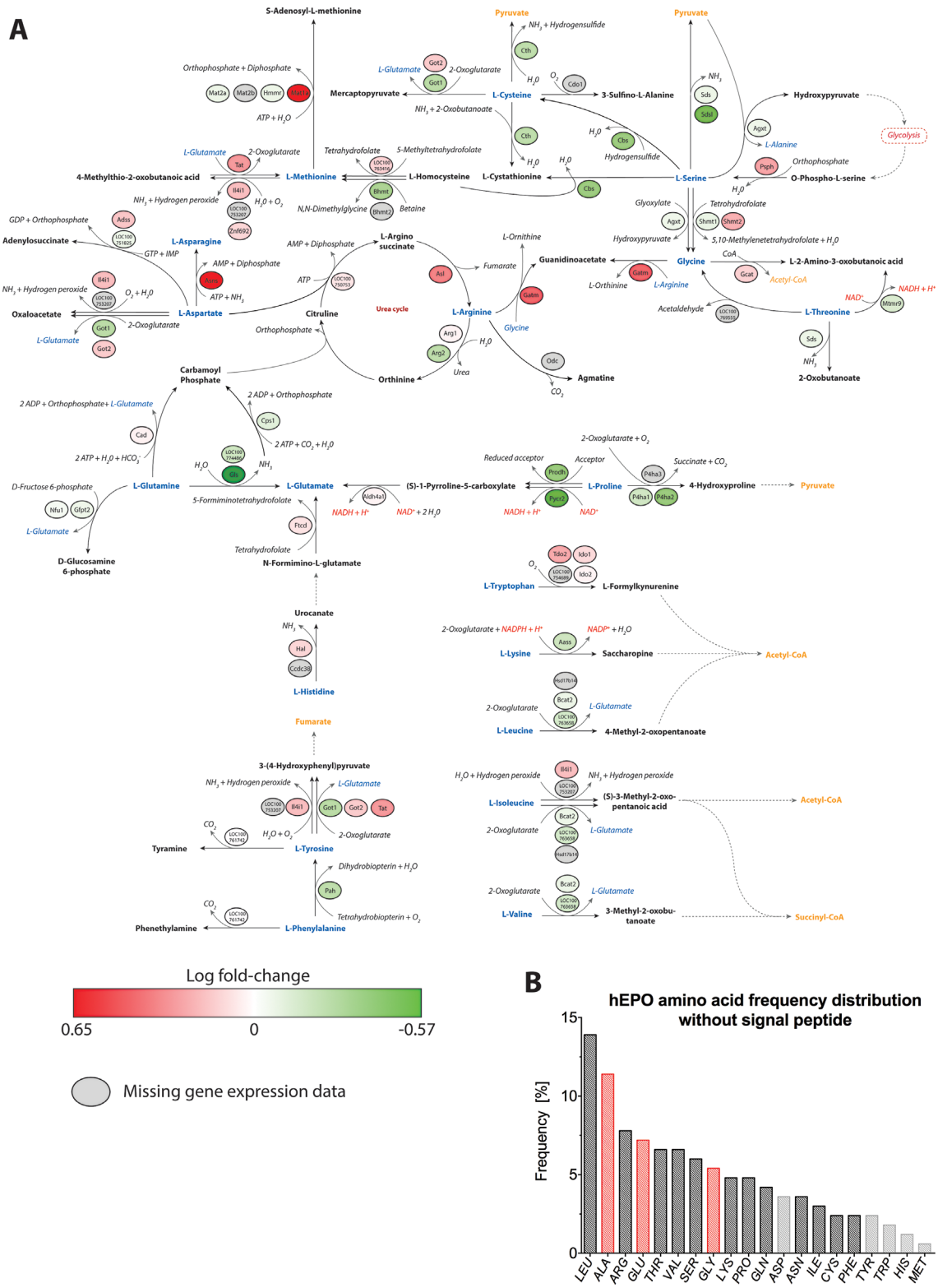

Figure 5. Differential gene expression analysis of amino acid catabolic genes in the high and low producer. **A**: Gene expression landscape of genes catalyzing the degradation or synthesis of amino acids. Circles indicate genes next to the reaction the encoded enzyme catalyzes. Gene expression values are shown as log fold-change indicating up- or down regulated genes in clone 7 relative to clone 1. Amino acids are colored blue, redox active metabolites are colored red and metabolites from the central metabolism are colored yellow. Reactions that do not produce or consume amino acids have been left out for simplicity. Dashed lines indicate multiple catalytic reactions. **B**: Frequency distribution of amino acids in human EPO without signal peptide. Black bars correspond to amino acids, which are preserved in clone 7 relative to clone 1. Gray bars indicate amino acids, which are not preserved. Red bars indicate amino acids that are secreted from the cells and therefore not considered in the analysis.

metabolic genes between the two EPO producing clones. The genes in the glycolytic pathway were generally up-regulated in the high producing clone, possibly reflecting an increased energy demand corresponding to the increased EPO productivity of this clone. That is, the normalization of growth rates in chemostat culture normalized the metabolic energy consumption from growth, thus allowing the quantification of energy requirement from heterologous protein production. Increased glycolytic flux in response to protein production during glucose-limited growth-restricted culture has been demonstrated in the eukaryotic production host *Pichia pastoris* (Heyland et al., 2010).

Heterologous Protein Production Causes Metabolic Changes in Favor of the Produced Protein

Heterologous protein production imposes a metabolic burden on the host cell metabolism, which causes redistribution of metabolic precursor fluxes to meet the increased anabolic demand for e.g. nucleotides for synthesis of RNA and activated sugar precursors associated with secretory protein production as shown by Niklas et al. (2013). The same study demonstrated that anabolic demand for nucleotide biosynthesis results in extracellular secretion of glycine and glutamate. Interestingly, we found that during steady state in chemostat culture, extracellular concentrations of glycine and glutamate were 1.8- and 2-fold higher in C7 relative to C1, respectively. This indicated that the secretion rates of glycine and glutamate increased with q_{EPO}, suggesting that the findings of Niklas et al. (2013) in human cells expressing α_1-antitrypsin are also valid for CHO cells expressing EPO.

The use of a nutrient-limited cultivation format restricts the possibility to increase nutrient uptake and inflict regulatory changes on cell metabolism, which may lead to flux-redistribution in favor of the heterologous protein. To further increase the knowledge on the adaptability of CHO cell metabolism, we performed a comparative transcriptome analysis of two clones with 25-fold differential EPO productivity in glucose-limited chemostat cultivations at $D = 0.3$ day^{-1}. Interestingly, we observed a change in the gene expression landscape of catabolic genes between the clones. The genes in the glycolytic pathway generally showed higher expression levels in the high producing clone, possibly reflecting an increased energy demand corresponding to the increased EPO productivity of this clone. Furthermore, the comparison of gene expression levels in the amino acid catabolism revealed a regulatory change around the amino acids, which are most abundant in EPO and not secreted from the cell. That is, the gene expression levels of enzymes producing these amino acids were generally up-regulated and expression levels of enzymes consuming the same amino acids were generally down-regulated in the high producer relative to the low producer (Fig. 5). This observation indicated a comparatively larger degree of metabolic adaptation to EPO production in the high producer, which may explain the larger increase of q_{EPO} in the high producer in phase III of chemostat culture (83% vs. 56% in high and low producers, respectively). Based on these data, we speculate that the amino acid metabolism in CHO cells may undergo adaptation in favor of the produced heterologous protein during long-term cultivation. The adaptation of gene expression levels in amino acid metabolism in favor of heterologous protein production during prolonged chemostat cultivation has been reported before in the eukaryotic protein production host *Saccharomyces cerevisiae* (Kazemi Seresht et al., 2013).

In conclusion, we provide evidence that EPO production up to 5 pg/cell/day is not limited by metabolism (i.e., glycolysis and associated energy metabolites) or bottlenecks in gene dosage, transcription and post-translational processing of EPO. Furthermore, we showed that glutamate and glycine secretion is increased in the high producing EPO clone, relative to the low producing clone, echoing the findings of Niklas et al. (2013) thus indicating possible anabolic demand for nucleotides and lipids, which could be candidate targets for medium supplementation to improve protein productivity.

Finally, we demonstrate that heterologous protein production can inflict metabolic changes in favor of the produced protein during prolonged chemostat cultivation. The observed adaptations of glycolysis and amino acid metabolism were followed by increased protein productivity in phase III (83% vs. 56% in high and low producers, respectively), suggesting that metabolic engineering of amino acid metabolism to reduce catabolism of amino acids present in the target protein could improve specific protein productivity in continuous culture. It was not possible to verify the reduced amino acid catabolism at the metabolite level using metabolic foot printing, thus future work should include quantification of intracellular levels of amino acid catabolic proteins or metabolic flux analysis to verify the suggested link between amino acid catabolism and heterologous protein production in chemostat culture.

We would like to thank Carsten Leisted, Jens Jacob Hansen, and Anja Kallesøe Pedersen for support with bioreactor cell culture experiments, cell line development and development of the HPLC-based EPO quantitation assay, respectively. H.F.K thanks the Novo Nordisk Foundation and the Lundbeck Foundation for financial support.

References

Andersen KB, von Meyenburg K. 1977. Charges of nicotinamide adenine nucleotides and adenylate energy charge as regulatory parameters of the metabolism in *Escerichia coli*. J Biol Chem 252(12):4151–4156.

Atkinson DE. 1968. Energy charge of the adenylate pool as a regulatory parameter. Interaction with feedback modifiers. Biochemistry 7(11):4030–4034.

Beckmann TF, Krämer O, Klausing S, Henrich C, Thüte T, Büntemeyer H, Hoffrogge R, Noll T. 2012. Effects of high passage cultivation on CHO cells: A global analysis. Appl Microbiol Biotechnol 94(3):659–671.

Bolt G, Kristensen C, Steenstrup TD. 2008. More than one intracellular processing bottleneck delay the secretion of coagulation factor VII. Thromb Haemost 100 (2):204–210.

Borth N, Mattanovich D, Kunert R, Katinger H. 2005. Effect of increased expression of protein disulfide isomerase and heavy chain binding protein on antibody secretion in a recombinant CHO cell line. Biotechnol Prog 21(1):106–111.

Bull AT. 2010. The renaissance of continuous culture in the post-genomics age. J Ind Microbiol Biotechnol 37(10):993–1021.

Choi YS, Lee DY, Kim IY, Kim HJ, Park HW, Choe TB, Kim IH. 2007. Enhancement of erythropoietin production in recombinant chinese hamster ovary cells by sodium lactate addition. Biotechnol Bioprocess Eng 12(1):60–72.

Chong WPK, Reddy SG, Yusufi FNK, Lee DY, Wong NSC, Heng CK, Yap MGS, Ho YS. 2010. Metabolomics-driven approach for the improvement of Chinese hamster ovary cell growth: Overexpression of malate dehydrogenase II. J Biotechnol 147 (2):116–121.

Chung JY, Lim SW, Hong YJ, Hwang SO, Lee GM. 2004. Effect of doxycycline-regulated calnexin and calreticulin expression on specific thrombopoietin productivity of recombinant chinese hamster ovary cells. Biotechnol Bioeng 85 (5):57.

Chusainow J, Yang YS, Yeo JHM, Toh PC, Asvadi P, Wong NSC, Yap MGS. 2009. A study of monoclonal antibody-producing CHO cell lines: What makes a stable high producer? Biotechnol Bioeng 102(4):1182–1196.

Dietmair S, Timmins NE, Gray PP, Nielsen LK, Krömer JO. 2010. Towards quantitative metabolomics of mammalian cells: Development of a metabolite extraction protocol. Anal Biochem 404(2):155–164.

Hammond S, Kaplarevic M, Borth N, Betenbaugh MJ, Lee KH. 2012. Chinese hamster genome database: An online resource for the cho community at www.CHOgenome.org. Biotechnol Bioeng 109:1353–1356.

Hansen BG, Salomonsen B, Nielsen MT, Nielsen JB, Hansen NB, Nielsen KF, Regueira TB, Nielsen J, Patil KR, Mortensen UH. 2011. Versatile enzyme expression and characterization system for *Aspergillus nidulans*, with the *Penicillium* brevicompactum polyketide synthase gene from the mycophenolic acid gene cluster as a test case. Appl Environ Microbiol 77(9):3044–3051.

Hayter PM, Curling EM, Baines AJ, Jenkins N, Salmon I, Strange PG, Tong JM, Bull AT. 1992. Glucose-limited chemostat culture of chinese hamster ovary cells producing recombinant human interferon-gamma. Biotechnol Bioeng 39 (3):327–335.

Hayter PM, Curling EM, Gould ML, Baines AJ, Jenkins N, Salmon I, Stange PG, Bull AT. 1993. The effect of the dilution rate on CHO cell physiology and recombinant interferon-gamma production in glucose-limited chemostat culture. Biotechnol Bioeng 42(9):1077–1085.

Heyland J, Fu J, Blank LM, Schmid A. 2010. Quantitative physiology of *Pichia pastoris* during glucose-limited high-cell density fed-batch cultivation for recombinant protein production. Biotechnol Bioeng 107(2):357–368.

Hung F, Deng L, Ravnikar P, Condon R, Li B, Do L, Saha D, Tsao YS, Merchant A, Liu Z, Shi S. 2010. MRNA stability and antibody production in CHO cells: Improvement through gene optimization. Biotechnol J 5(4):393–401.

Hussain H, Maldonado-Agurto R, Dickson AJ. 2014. The endoplasmic reticulum and unfolded protein response in the control of mammalian recombinant protein production. Biotechnol Lett 36(8):1581–1593.

Hwang SO, Chung JY, Lee GM. 2003. Effect of doxycycline-regulated ERp57 expression on specific thrombopoietin productivity of recombinant CHO cells. Biotechnol Prog 19(1):179–184.

Jayapal K, Wlaschin K. 2007. Recombinant protein therapeutics from CHO cells-20 years and counting. Chem Eng Prog 103(10):40–47.

Jiang Z, Huang Y, Sharfstein ST. 2006. Regulation of recombinant monoclonal antibody production in chinese hamster ovary cells: A comparative study of gene copy number, mRNA level, and protein expression. Biotechnol Prog 22 (1):313–318.

Jossé L, Smales CM, Tuite MF. 2012. Engineering the chaperone network of CHO cells for optimal recombinant protein production and authenticity. Methods Mol Biol 824:595–608.

Kanehisa M, Goto S. 2000. KEGG: Kyoto encyclopedia of genes and genomes. Nucleic Acids Res 28(1):27–30.

Kanehisa M, Goto S, Sato Y, Kawashima M, Furumichi M, Tanabe M. 2014. Data, information, knowledge and principle: Back to metabolism in KEGG. Nucleic Acids Res 42:D199–D205.

Kang S, Ren D, Xiao G, Daris K, Buck L, Enyenihi AA, Zubarev R, Bondarenko PV, Deshpande R. 2014. Cell line profiling to improve monoclonal antibody production. Biotechnol Bioeng 111(4):748–760.

Kazemi Sereshy A, Cruz AL, de Hulster E, Hebly M, Palmqvist EA, van Gulik W, Daran JM, Pronk J, Olsson L. 2013. Long-term adaptation of *Saccharomyces cerevisiae* to the burden of recombinant insulin production. Biotechnol Bioeng 110(10):2749–2763.

Khoo SHG, Falciani F, Al-Rubeai M. 2007. A genome-wide transcriptional analysis of producer and non-producer NS0 myeloma cell lines. Biotechnol Appl Biochem 47(Pt 2):85–95.

Kildegaard HF, Baycin-Hizal D, Lewis NE, Betenbaugh MJ. 2013. The emerging CHO systems biology era: Harnessing the 'omics revolution for biotechnology. Cur Opin Biotechnol 24(6):1102–1107.

Kim YG, Lee GM. 2009. Bcl-xL overexpression does not enhance specific erythropoietin productivity of recombinant CHO cells grown at 33 degrees C and 37 degrees C. Biotechnol Prog 25(1):252–256.

Kim J, Lee Y, Kim H, Chang KH, Kim JHOE, Kim HJ. 2004. Enhancement of erythropoietin production from chinese hamster ovary (cho) cells by introduction of the urea cycle enzymes, carbamoyl phosphate synthetase I and ornithine transcarbamylase. J Microbiol Biotechnol 14 (4):844–851.

Kim Y-G, Kim JY, Park B, Ahn JO, Jung JK, Lee HW, Lee GM, Lee EG. 2011. Effect of Bcl-xL overexpression on erythropoietin production in recombinant Chinese hamster ovary cells treated with dimethyl sulfoxide. Process Biochem 46 (11):2201–2204.

Kim JY, Kim Y-G, Lee GM. 2012. CHO cells in biotechnology for production of recombinant proteins: Current state and further potential. Appl Microbiol Biotechnol 93(3):917–930.

Lattenmayer C, Loeschel M. 2007. Protein-free transfection of CHO host cells with an IgG-fusion protein: Selection and characterization of stable high producers and comparison to conventionally transfected clones. Biotechnol Bioeng 96 (6):1118–1126.

Lattenmayer C, Trummer E, Schreibl K, Vorauer-Uhl K, Mueller D, Katinger H, Kunert R. 2007. Characterisation of recombinant CHO cell lines by investigation of protein productivities and genetic parameters. J Biotechnol 128(4):716–725.

Lee FW, Elias CB, Todd P, Kompala DS. 1998. Engineering Chinese hamster ovary (CHO) cells to achieve an inverse growth—Associated production of a foreign protein, beta-galactosidase. Cytotechnology 28(1–3):73–80.

Lee CJ, Seth G, Tsukuda J, Hamilton RW. 2009a. A clone screening method using mRNA levels to determine specific productivity and product quality for monoclonal antibodies. Biotechnol Bioeng 102(4):1107–1118.

Lee YY, Wong KTK, Tan J, Toh PC, Mao Y, Brusic V, Yap MGS. 2009b. Overexpression of heat shock proteins (HSPs) in CHO cells for extended culture viability and improved recombinant protein production. J Biotechnol 143:34–43.

Lund AM, Kildegaard HF, Petersen MBK, Rank J, Hansen BG, Andersen MR, Mortensen UH. 2014. A versatile system for USER cloning-based assembly of expression vectors for mammalian cell engineering. PLoS ONE 9(5):396693.

Mason M, Sweeney B, Cain K, Stephens P, Sharfstein ST. 2012. Identifying bottlenecks in transient and stable production of recombinant monoclonal-antibody sequence variants in Chinese hamster ovary cells. Biotechnol Prog 28 (3):846–855.

Mead EJ, Chiverton KM, Smales CM, von der Haar T. 2009. Identification of the limitations on recombinant gene expression in CHO cell lines with varying luciferase production rates. Biotechnol Bioeng 102(6):1593–1602.

Mohan C, Lee GM. 2010. Effect of inducible co-overexpression of protein disulfide isomerase and endoplasmic reticulum oxidoreductase on the specific antibody productivity of recombinant Chinese hamster ovary cells. Biotechnol Bioeng 107 (2):337–346.

Niklas J, Priesnitz C, Rose T, Sandig V, Heinzle E. 2013. Metabolism and metabolic burden by alpha1-antitrypsin production in human AGE1.HN cells. Metab Eng 16(1):103–114.

Nyberg GB, Balcarcel RR, Follstad BD, Stephanopoulos G, Wang DI. 1999. Metabolism of peptide amino acids by Chinese hamster ovary cells grown in a complex medium. Biotechnol Bioeng 62(3):324–335.

O'Callaghan PM, McLeod J, Pybus LP, Lovelady CSW, Stephen J, Racher AJ, Porter A, James DC. 2010. Cell line-specific control of recombinant monoclonal antibody production by CHO cells. Biotechnol Bioeng 106(6):938–951.

Peng R-W, Fussenegger M. 2009. Molecular engineering of exocytic vesicle traffic enhances the productivity of Chinese hamster ovary cells. Biotechnol Bioeng 102(4):1170–1181.

Peng R-W, Abellan E, Fussenegger M. 2011. Differential effect of exocytic SNAREs on the production of recombinant proteins in mammalian cells. Biotechnol Bioeng 108(3):611–620.

Powell J, Berkner K. 1986. Human erythropoietin gene: High level expression in stably transfected mammalian cells and chromosome localization. Proc Natl Acad Sci USA 83:6465–6469.

Pybus LP, Dean G, West NR, Smith A, Daramola O, Field R, Wilkinson SJ, James DC. 2013. Model-directed engineering of "difficult-to-express" monoclonal antibody production by Chinese hamster ovary cells. Biotechnol Bioeng 111 (2):372–385.

Regenberg B, Grotkjær T, Winther O, Fausbøll A, Åkesson M, Bro C, Hansen LK, Brunak S, Nielsen J. 2006. Growth-rate regulated genes have profound impact on interpretation of transcriptome profiling in *Saccharomyces cerevisiae*. Genome Biol 7(11):R107.

Reisinger H, Steinfellner W, Stern B, Katinger H, Kunert R. 2008. The absence of effect of gene copy number and mRNA level on the amount of mAb secretion from mammalian cells. Appl Microbiol Biotechnol 81(4):701–710.

Sellick C A, Knight D, Croxford AS, Maqsood AR, Stephens GM, Goodacre R, Dickson AJ. 2010. Evaluation of extraction processes for intracellular metabolite profiling of mammalian cells: Matching extraction approaches to cell type and metabolite targets. Metabolomics 6(3):427–438.

Sengupta N, Rose ST, Morgan J A. 2011. Metabolic flux analysis of CHO cell metabolism in the late non-growth phase. Biotechnol Bioeng 108(1):82–92.

Smales CM, Smales CM, Dinnis DM, Stansfield SH, Alete D, Sage EA, Birch JR, Racher AJ, Marshall CT, James DC. 2004. Comparative proteomic analysis of GS-NS0 murine myeloma cell lines with varying recombinant monoclonal antibody production rate. Biotechnol Bioeng 88(4):474–488.

Sung KY, Jong KH, Gyun ML. 2004. Effect of simultaneous application of stressful culture conditions on specific productivity and heterogeneity of erythropoietin in Chinese hamster ovary cells. Biotechnol Prog 20(4):1293–1296.

Surabattula R, Rao KRSS, Polavarapu R. 2011. An optimized process for expression, scale-up and purification of recombinant erythropoietin produced in chinese hamster ovary cell culture. Res Biotechnol 2(3):58–74.

Untergasser A, Cutcutache I, Koressaar T, Ye J, Faircloth BC, Remm M, Rozen SG. 2012. Primer3-new capabilities and interfaces. Nucleic Acids Res 40(15):e115.

Walsh G 2014. Biopharmaceutical benchmarks 2014. Nat Biotechnol 32(10):992–1000.

Yee JC, Gerdtzen ZP, Hu W-S. 2009. Comparative transcriptome analysis to unveil genes affecting recombinant protein productivity in mammalian cells. Biotechnol Bioeng 102(1):246–263.

Yoon SK, Song JY, Lee GM. 2003. Effect of low culture temperature on specific productivity, transcription level, and heterogeneity of erythropoietin in Chinese hamster ovary cells. Biotechnol Bioeng 82(3):289–298.

Yoon SK, et al. 2005. Effect of culture pH on erythropoietin production by Chinese hamster ovary cells grown in suspension at 32.5 and 37.0 degrees C. Biotechnol Bioeng 89(3):345–356.

Zhou H, et al. 2010. Generation of stable cell lines by site-specific integration of transgenes into engineered Chinese hamster ovary strains using an FLP-FRT system. J Biotechnol 147(2):122–129.

Supporting Information

Additional supporting information may be found in the online version of this article at the publisher's web-site.